LAWRENCE
LIVERMORE
NATIONAL
LABORATORY

UCRL-CONF-211435

Hazards Response of Energetic Materials - Developing a Predictive Capability for Initiation and Reaction under Multiple Stimuli

A. L. Nichols III, B. K. Wallin, J. L. Maienschein, J. E. Reaugh, J. J. Yoh, M. E. McClelland

April 15, 2005

36th International ICT-Conference & 32nd International Pyrotechnics Seminar
Karlsruhe, Germany
June 28, 2005 through July 1, 2005

Hazards Response of Energetic Materials – Developing a Predictive Capability for Initiation and Reaction under Multiple Stimuli

Albert L. Nichols III, Bradley K. Wallin, Jon L. Maienschein,
John E. Reaugh, J. Jack Yoh, Matthew E. McClelland
Lawrence Livermore National Laboratory
Livermore, CA 94551

Abstract

We present our approach to develop a predictive capability for hazards – thermal and non-shock impact – response of energetic material systems based on: A) identification of relevant processes; B) characterization of the relevant properties; C) application of property data to predictive models; and D) application of the models into predictive simulation. This paper focuses on the last two elements above, while a companion paper by Maienschein *et al* focuses on the first two elements. We outline models to describe the both the microscopic evolution of hot spots for detonation response and thermal kinetic models used to model slow heat environments. We show examples of application to both types of environments.

I. Introduction

Predicting the response of energetic materials to complex stimuli is of critical importance in order to understand the safety characteristics of systems containing energetic materials. The energetic material system may be subject to a wide variety of insults that in principle need to be characterized. The breadth of these scenarios compels the need for the development of fundamental models for energetic material response. It is the hope that such development can reduce the need for full scale experiments by both pinpointing the material properties needed for the model and integrating this information in a manner that can be used to quantify our uncertainty.

Our goal is to develop a predictive capability for hazards response of energetic material systems based on: A) identification of the relevant processes in chemical reaction, heat flow, and material motion that govern the hazards response; B) characterization of the relevant properties of the energetic material; C) application of these data to develop predictive mathematical models of the material behavior; and D) incorporation of the models into modern high-fidelity computer codes to allow predictive simulation of the behavior of actual systems containing these materials. This paper will focus the last two elements. A companion paper by Maienschein et al discusses the overall approach.

The basic characteristic of all energetic materials is that they are capable of the release of large quantities of energy. However, the conditions under which this energy may be released must be relatively difficult to attain, otherwise they would be too difficult to handle. This has direct implications on the kinds of mechanisms that need to be considered in the energetic material model. Intrinsically, these mechanisms are connected to the thermally driven chemical reactions of the energetic material. Thus, in order to model the energetic response, consideration must be given to how energy flows in the system, both locally and globally. Local energy focusing, known as hot spots, are key to the understanding the initiation response of mechanical insults. We have developed and will present a statistical hot spot model that elucidates the processes involved with mechanical driven initiation. Global heat flow is central to the understanding thermal explosion.

Once the energetic material has begun to react, the hazard associated with it is determined by the rate at which it releases energy. For thermal explosion, this is dependent on the level of preconditioning of the explosive. We have developed models to account for the change in state and condition of the material during the long pre-ignition phase, and then the effect these changes have on the subsequent deflagration. For mechanical driven ignition, the number and type of hot spots determines the level of violence. We are currently developing model frameworks that can be used to incorporate the effects of damage on the creation and destruction of potential hot spots by thermal and mechanical preconditioning.

All of these models have been incorporated into a modern coupled thermal-mechanical-chemical hydro-code, and we will show its application of these models to sample problems.

In Section II we describe the ALE3D code and define NLTE SHS model. In Section III we describe the process for defining the parameters used in our models. In Section IV we show results of the model as applied to detonation and cookoff, and summarize in Section V.

II. The ALE3D Code and NLTE SHS Model

The ALE3D[1,2] code is a coupled thermal-hydro-chemical code that has been under development at LLNL for several years. The current version of ALE3D began as a 3D ALE hydrocode to which has been added several capabilities. These include implicit thermal transport, thermally driven reactions, models for both the thermal and mechanical properties of chemical mixtures, second order species advection, and implicit hydrodynamics.

Probabilistic hot spot Formulation

Nichols and Tarver[3] initially described the statistical hot spot formulation. The first phase in constructing the statistical hot spot model is the consideration of the distribution of those hot spots. The model assumes that potential hot spots are randomly distributed in space. When a stimulus arrives, the potential hot spots can either be ignited or destroyed (e.g. enough energy is localized in the hot spot to induce a self sustained reaction, or energy dissipation removes the energy faster than the reaction can start.) Once ignited, we assume that the hot spots either grow radially with a burn rate $v(P)$, which is defined as a function of the local pressure. We define the number of hot spots that are active at time t is $\bar{\rho}_A(t)$, and $\rho_B(t)$ as the number of hot spots created at time t. In the current model, it is assumed that all hot spots active at time t have the same rate of death $\mu(t)$. With these assumptions, the log of the extent of reaction *h* can be related to the ignition rate with the following differential equations:

$$\begin{aligned}
\frac{\partial h}{\partial t} &= 4v(t)\bar{g}(t) + 4\pi\varepsilon^3\rho_B(t)/3 \\
\frac{\partial \bar{g}}{\partial t} &= \pi v(t)\bar{f}(t) + 4\pi\varepsilon^2\rho_B(t) - \mu(t)\bar{g}(t) \\
\frac{\partial \bar{f}}{\partial t} &= 2v(t)\bar{\rho}_A(t) + 2\varepsilon\rho_B(t) - \mu(t)\bar{f}(t) \\
\frac{\partial \bar{\rho}_A}{\partial t} &= \rho_B(t) - \mu(t)\bar{\rho}_A(t)
\end{aligned} \tag{1}$$

where ε is initial hot spot size, and where *f* and *g* are intermediate components whose definition we will not pursue here.

An ignition model is needed to define $\rho_B(t)$. We begin by defining the initial density of potential hot spots ρ_P^0.The following phenomenological ignition model that captures many of the features required of an ignition model is:

$$\mathrm{K}(p) = \left(\frac{AP^*(p - P_0)}{P^* + p - P_0}\right) H(p - P_0) \tag{2}$$

$$\begin{aligned}
\dot{\rho}_P &= -\rho_P \mathrm{K}(p) \\
\rho_B &= \rho_P(\mathrm{K}(p) - \mathrm{K}(P_A))H(\mathrm{K}(p) - \mathrm{K}(P_A))
\end{aligned} \tag{3}$$

Here K(p) is the rate of potential hot spot transformation, and $K(P_A)$ is the constant death rate for potential hot spots. It is the rate of transformation at the pressure P_A when the first hot

spots actually start igniting. P_0 is the ignition rate threshold pressure that represents the internal resistance to void collapse. To prevent unrealistically large collapse rates during numerical pressure spikes, P^* is defined as the saturation pressure. H is the heavy side step function, which is zero for all arguments less than zero and one for everything else. We originally envisioned a compression rate dependent ignition rate, but such a rate can be extremely mesh-size dependent. More complex ignition models can be formulated as this model evolves.

Table 1. Reaction Rate Parameters for NLTE SHS Model

Parameter	***Model 1***	***Model 2***
P_0 (GPa)	0.6	0.6
P_A(GPa)	1.2	1.2
P^*(GPa)	10	10
Void Fraction	0.02	0.02
$\tau(\mu s)$	0.009	0.009
ε (cm)	8.6358E-06	1.0531e-4
ρ_P^0 (cm^{-3})	7.4127E+12	4.0871e9
A (cm-μs/g)	51741.	4242.8
$D(\mu s^{-1})$	292.88	24.016
μ (μs^{-1})	1	1
Pressure (GPa)	***Burn Rate (cm/μs***	
0.0001	2.35E-07	2.35E-07
0.1	1.00E-05	1.00E-05
3.	4.00E-04	5.00E-04
7.5		2.50E-03
10		4.00E-03
15.		9.00E-03
20	2.85E-3	
37.	4.1E-3	5.00E-02
100.		5.00E-02
200	1.6E-2	

Non-Local Thermodynamic Equilibrium Material model

For the hot spot model, we use a non-local thermodynamic model for the equation of state of the mixture of reactants and products. In our model, the extent of composition change and the hydrodynamic work are conducted simultaneously and self consistently. As the reactant transforms into products, the internal energy and volume are exchanged along with the mass fractions in a time centered self consistent manner. Energy is advanced through pdv work for each species and the material as a whole using a third order Runge-Kutta scheme. In our current model, we assume that any external energy and q^edv work associated with the artificial viscosity in the zone is distributed equally to each species by their mass. The pressure used to determine the reaction rate is taken to be the average of the pressure at the beginning and end of the time step. The relative volume of each component is adjusted until pressure and extent of reaction have been equilibrated.

III. Model Parameterization

Parameters for the NLTE SHS Model

For the NLTE SHS model, we have defined a total of 8 parameters, not counting those associated with the equation of state, for the statistical hot spot model. They are: P_0, P^*, A, μ, v, P_A, ρ_P^0, and ε. P_0 is related to the yield strength of the explosive, and so we will use the yield strength in our model. The burn velocity v is derived from strand-burner and diamond

anvil experiments. The value of P_A is set equal to the value of the shock pressure that just begins to ignite the explosive.

The values of ρ_P^0, ε, A, and P^* are determined by a heuristic arguments relating them to the total initial hot spot volume, burn rate v at the detonation pressure p_D, the reaction zone time τ, initial void density ρ_v, the rate of pore collapse under pressure:

$$\begin{aligned} \rho_v &\approx 4\pi\varepsilon^3 \rho_P^0 / 3 \\ \rho_A^0 &\approx \rho_P^0 \left[1 - K(P_A)/K(p_D)\right] \\ 1 &\approx 4\pi(\varepsilon + v\tau)^3 \rho_A^0 / 3 \end{aligned} \qquad A \approx \frac{1}{(2\varepsilon\rho_0 c)}$$

where ρ_0 is the initial density, and c is the reference sound speed. We can handle the natural curvature that comes out of this formulation by an appropriate choice of P^*.

Reactant and product equations of state are needed to describe the states attained during shock compression. The Jones-Wilkins-Lee (JWL) equation of state is used for the reactant with typical parameters for an HMX-based plastic bonded explosive. This JWL equation fits the measured reactant Hugoniot data at low shock pressures and the von Neumann spike data at high pressures[4]. The reaction products are described by LEOS tables fit to product equation of state calculated by the CHEETAH chemical equilibrium code[5].

Parameters for Slow Heat Enviornments

ALE3D chemical, mechanical, and thermal models have been developed to model the cookoff of LX-10 in the Scaled Thermal EXplosion (STEX)[6] test. The decomposition of HMX in the LX-10 is modeled by four-step, five-species chemical kinetics based on the model reported in [7]. The first two steps are endothermic and the final two steps are exothermic. The components are the solid species β- and δ-HMX, a solid intermediate, and intermediate and final gas products. The decomposition of Viton A is represented by a single-step endothermic reaction. The two reactions sequences are treated as non-interacting.

After the Arrhenius reaction rates have increased to the point where changes are occurring on the time scale of sound propagation, a switch is made to a burn front model in which reactants are converted to products in a single reaction step. We assume that the burn front velocity, V, is a function of the pressure, P, at the front location, and use piece-wise power-law expressions of the form to describe segments of the burn front curve. The deflagration rate of LX-10 was measured with the LLNL High Pressure Strand Burner

The mechanical behavior of the condensed HE constituents along with the Viton reactant is represented by Steinberg-Guinan mechanical models with a 7-term polynomial equation of state. The constant volume heat capacity does not vary with temperature in this EOS. Calculated melt and cold curves are used to account for the influence of compression on melting energy. A nonlinear regression[8] procedure was used to determine the coefficients that give an optimal representation of the measurements of the thermal expansion, compressibility, sound speed, and the unreacted shock Hugoniot. The model gas constituents along with the air in the gap are treated as no-strength materials with gamma-law equations of state.

The time-dependent thermal transport model includes the effects of conduction, reaction, advection, and compression. The constant-volume heat capacity is constant for each reactant consistent with the Steinberg-Guinan model. The thermal conductivity for the condensed species is taken to be constant, whereas the effects of temperature are included for the gaseous species. The heat capacity for the gases is assigned the same constant-volume value used in the gamma-law model. The temperature-dependent thermal conductivity is estimated at 1 kbar (100 MPa) using Bridgman's[9] equation for liquids in which the sound velocity is calculated using results from CHEETAH.

IV. Results

NLTE SHS Model for PBX-9501 Detonation Velocity Diameter Effect

As discussed in the previous section, the ignition and growth of reaction model has eight parameters: P_0, P^*, A, μ, v, P_A, ρ_P^0, and ε. The parameters for the model developed here are listed in Table 1. P_0 is the ignition rate threshold pressure and is set to the Hugoniot elastic limit for HMX[10]. The activation threshold has been set to twice the Hugoniot elastic limit. The reaction growth rate v is assumed to be a function of pressure as measured experimentally in strand burner[11] and diamond anvil cells on pure HMX[12]. This pressure versus burn rate function is shown in Table 1. The initial hot spot diameter ε and initial number of potential hot spot sites ρ_P^0 are derived from the burn rate at the detonation conditions based on a reaction time set to match experimental results.

We examine the detonation velocity diameter effect with the statistical hot spot model. In order to determine the detonation velocity, two-dimensional axi-symmetric problems at the requisite diameters were created. The length to diameter ratio was set to 4, and the calculation was run for 10 microseconds times the radius in cm. This generally ensured that the shock

wave has proceeded through approximately 90% of the length. The cylinder of explosive was given a velocity of .1 mm/microsecond into unmovable stonewall. A mesh resolution of 1000 elements per cm was used for most of the work shown here. Multiple resolutions were used to confirm mesh convergence. In order to capture the locus of the detonation front, the cylinder was divided into two regions, one a single element thick running along the axis. The location of the highest pressure in this region was then written to a history file for processing. The detonation velocity was calculated by a least squares fit to the final eighth of the time steps.

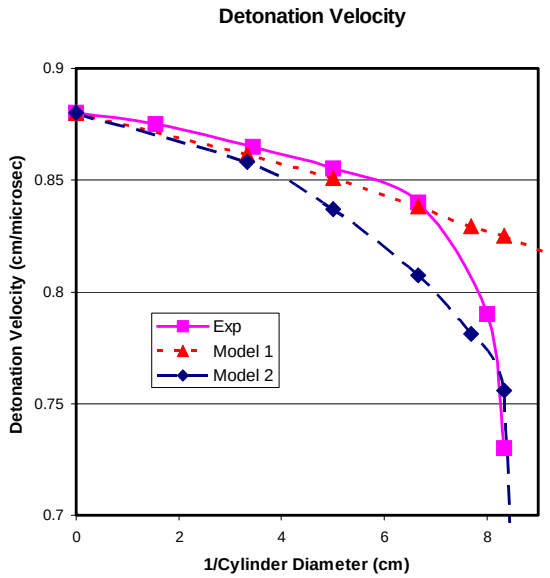

Figure 1. Detonation Velocity as a function of inverse cylinder diameter. The solid square dots are the experimental results of Campbell and Engelke. Model 1 has a explosive burn rate exponent of approximately 0.75, while model two has a higher exponent above 3 GPa.

Two models are shown in Table 1. The first model developed uses a burn rate pressure exponent of ~0.75 that essentially matches the experimental data. The second model follows the higher-pressure burn rate and then continues with an exponent of 2 to the detonation pressure. The detonation velocity versus cylinder diameter for both models and the experimental results of A. W. Campbell and Ray Engelke[13] are plotted in Figure 1. Although model 1 reproduces the detonation velocity diameter effect for large diameters, the detonation continues to propagate even at small diameters, contrary to experimental observation. This behavior is typical of all reaction models that use a pressure burn rate exponent of 0.75. Essentially, the burn rate does not change rapidly enough to cause the classical detonation failure, but instead the detonation velocity steadily drops until it merges with the sound speed. The fact that this model does not properly fail at small diameters leads one to believe that there are processes that are not being captured in this model.

One issue that could affect the model is the burn rate function. The experimental data that we use was collected at room temperature. Although the burn rate tends to exhibit weak temperature dependence, temperature changes in the order of a thousand degrees will

probably result in significant change in the burn rate. An effective burn rate with a higher-pressure exponent would represent the temperature increased burn rate, since the temperature increases as we increase the shock pressure. This is the basis of model 2. Model 2 slightly under predicts the detonation velocity in the intermediate diameters until just before detonation failure. The model does reproduce the classic detonation failure diameter.

Slow Heat results for Scalable Thermal EXplosion Test of LX-10

The STEX apparatus, shown in Figure 2, consists of a 8 inch long, 2 inch diameter thin walled vessel with 1 inch flanges and base plates to provide stout end confinement. A two-dimensional, axisymmetric ALE3D model is used to simulate the cookoff of LX-10 in STEX Test TE-047. In the experiment, the system includes 8.66% by ullage by volume distributed over the sides and ends. In the simulation, the ullage is applied entirely to the sides to minimize the artificial pressurization resulting from numerical artifacts associated with the modeling of the gap. The gap is filled with air described by a gamma-law model in which the constant volume heat capacity is increased by a factor of 10 above its physical value to reduce spurious temperature increases associated with rapid compression. All components of the vessel assembly are taken to be perfectly joined.

The top, bottom, and side heaters are applied as uniform heat flux conditions on the top, bottom, and side surfaces. Included among the side heater surfaces are the sides of the tube and flanges along with the inward facing surfaces of the flanges. The heat fluxes for these

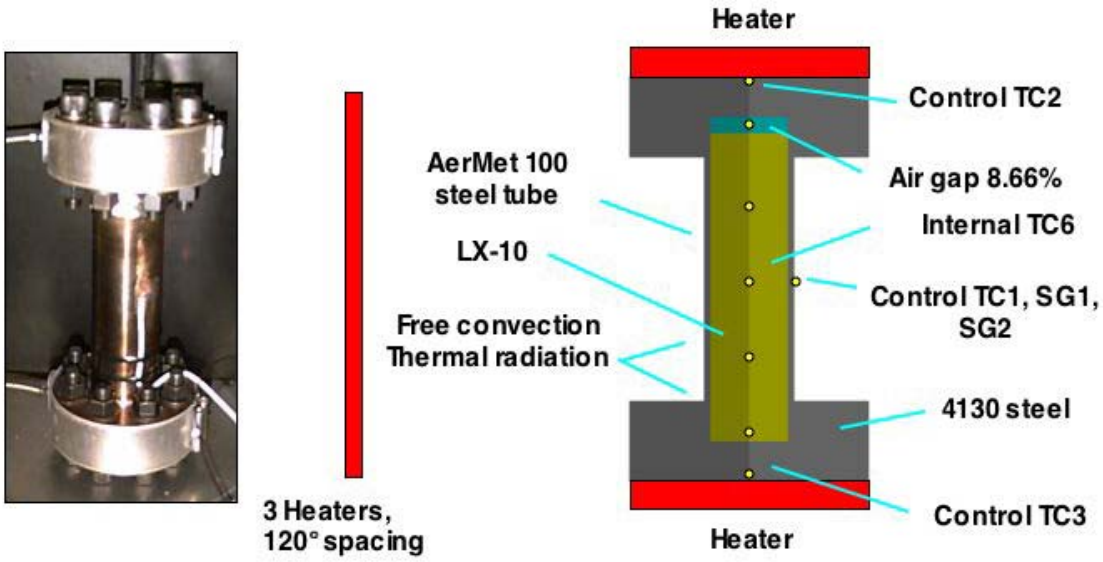

Figure 2. Schematic for STEX test with LX-10 confined in an AerMet 100 vessel.

three heaters are adjusted using three independent PI controllers to maintain the temperatures at the cylinder mid plane (TC1), and top (TC2), and bottom (TC3) at their set-point values. Thermal convection is applied to all outward facing surfaces using heat transfer coefficients for laminar flow of air past appropriate model surfaces such as vertical and horizontal plates[14]. Standard expressions for hemispherical radiation are used on these same surfaces. A boundary layer expression for heat transfer resulting from the flow of air past a vertical plate is used on the tube surface. This expression has a dependence on the vertical coordinate, and is used to compensate for preferential cooling observed on the lower portion of the tube. During the final ramp of 1° C/h, the upper and lower control temperatures TC2 and TC3 are kept 9 and 5°C cooler than the side control temperature in an attempt to keep the ignition point near the axial midplane .

The ALE3D computer code requires 3D meshes, and a wedge-shaped mesh is employed for the 2D model of this study. A small hole is present near the symmetry axis to allow the use of hexahedral elements at all locations. In the base case, the tube cavity has 12 elements in the radial direction which is increased by a factor of 2 in mesh refinement studies. Some of the elements have both HE and air, and standard mixing rules are employed to calculate the energy, heat capacity, thermal conductivity, shear modulus, and equation of state[15]. The mesh is smoothed using a combination of Lagrange and Eulerian algorithms. Nodes initially on the interface between the cavity and the steel remain on these boundaries while nodes interior to the cavity are advected through the flowing HE and air.

A fully implicit method is used for the integration of the thermal transport equations during the thermal ramp and much of the subsequent ignition process. During the thermal ramp and subsequent ignition process, the hydrodynamic equations are integrated using an explicit method with the material densities increased by a large factor to make the calculations computationally feasible. An algorithm is used to select the scale factor. During thermal runaway, the time step is decreased by approximately 14 orders of magnitude to resolve behavior on the dramatically shrinking time scale.

After a temperature reaches a user-specified threshold value, the multi-step kinetics model is replaced by the burn front model that propagates through the HE converting reactants to products in a single step. This burn front is tracked using a level set method that conserves mass, momentum, and energy across the front. Since the mesh is not moved to explicitly track the front, the resolution of the burn front is on the scale of the mesh element size.

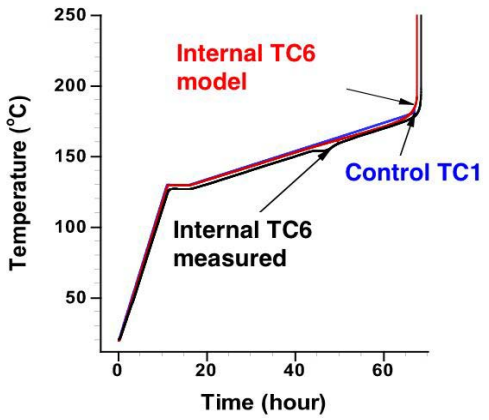

Figure 3. Measured and ALE3D model temperature results for STEX test TE-047 with LX-10

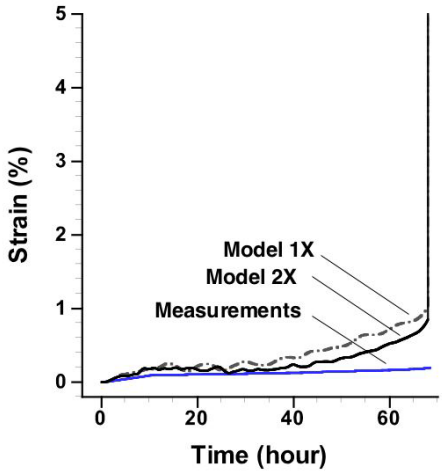

Figure 4. Comparison of model and measured strain rates for STEX test TE-047 with LX-10

Comparison of Model and Measured Cookoff Results for LX-10

In cookoff Test TE-047 for LX-10, the set-point temperature for TC1 was increased in stages from room temperature to 130°C, held for 5.0 h, and then increased at 1°C/h until thermal runaway. The measured center internal temperature (TC6) shows a dip around 152 °C which is believed to be associated with the beta to delta phase transition for HMX. After the hold at 130°C, the top and bottom set-point temperatures TC2 and TC3 are kept 9°C and 4°C cooler than TC1, respectively. The cookoff temperature, taken to be the set-point temperature at the end of runaway, is 182 °C for both the simulation and experiment, indicating that the model provides an excellent prediction (Figure 3). Both the measured and model internal temperatures begin to increase 2 h before ignition.

Initial experimental and model hoop strain results for the rapid expansion are shown for the duration of the test in Figure 4. The location for the measurement is the side of the vessel at the axial midplane. On the 70 h time scale of the test, the strain measured on long times shows linear increases that follow the changes in temperature. This suggests that the increases in measured strain follow the thermal expansion of the tube. At ignition, there is a rapid increase in strain to 3.4% based on the measurements at a high sampling rate (not shown). The simulated strains for the 1X and 2X meshes, approximately track the measured values until t=40 h at which time there is a more rapid increase in the model curves. The model results are approaching the measured results as the mesh is refined. The discrepancies observed are likely the result of the model representation of the gap using mixed materials, and possibly flaws in the chemical kinetics models as has been noted in earlier studies[16,17]. In

the future, more detailed comparisons will be made between model calculations and the measured strains, the PDV curves, and radar measurements described.

V. Summary

In this paper, we have described a new detonation model for HMX. The equations of state models are based on current best practice. The reaction parameters have been based available reactant experimental data. The mixture equation of state equilibrates the pressure of each species, but does not equilibrate the temperature. Instead, we track the flow of energy as the composition changes from one species to another. This keeps the reactants cold while the products will be hot, in keeping with the physical model. These models were applied to the detonation velocity diameter effect, to good result.

ALE3D models were applied to the STEX test with LX-10 confined in an AerMet 100 tube. The mechanical behavior of the AerMet 100 was represented by Steinberg-Guinan models with a Gruneisen EOS. A Steinberg-Guinan mechanical model with polynomial EOS was used for the HMX and Viton solid species while Gamma-Law models were selected for the gases. A four-step Tarver-McGuire model was used to represent the chemical kinetics behavior at long times based on ODTX measurements. The power-law burn model was employed for the microsecond time to represent measurements made with the high-pressure-strand burner. The prediction for the explosion temperature was in excellent agreement with the measured value. However, the predicted strains were significantly larger than the measured values. The numerical errors are expected to be reduced with the addition of implicit integration for the momentum equation which is currently in development, and improved modeling of the internal porosity of the material.

The results shown here describe the process that we have begun to use to model the response of energetic materials to a variety of hazard conditions. These models are integrated within a single modern code framework, which allows us to use the appropriate models as needed. In the future we plan to more tightly couple these models so that the code will naturally transition from the slow thermal to fast thermal to impact loading to shock loading without the need of the user to define a separate model for each process.

VI. Acknowledgments

We would like to acknowledge the contributions of our colleagues at US DOE and DoD laboratories, as well as colleagues in Europe, with whom we have had many discussions over

the last several years, and funding from the Joint DOD-DOE Munitions Technology Program. This work was performed under the auspices of the U.S. Department of Energy by University of California, Lawrence Livermore National Laboratory under Contract W-7405-Eng-48.

References:

1. Dube, E., Neely, R., Nichols, A., Sharp, R., Couch , R., & The ALE3D Team, "Users Manual for ALE3D An Arbitrary Lagrange/Eulerian 3D Code System, Version 3.2.0" , Internal Publication, Lawrence Livermore National Laboratory, Livermore, CA. (2002).
2 Nichols, A. L., Anderson, A., Neely, R. and Wallin, B. "A Model for High Explosive Cookoff," in Proceedings of 12th International Detonation Symposium, San Diego, CA, (2002).
3. Nichols, A. L., III, and Tarver, C. M., "A Statistical Hot Spot Reactive Flow Model for Shock Initiation and Detonation of Solid High Explosives", presented at Twelfth International Detonation, San Diego, CA, 2002.
4. Tarver, C. M., Urtiew, P. A., Chidester, S. K., and Green, L. G., Propellants, Explosives, Pyrotechnics 18, 117 (1993).
5. Fried, L., Howard, W. M., and Souers, P. C., presented at Twelfth International Detonation, San Diego, CA, 2002.
6 Maienschein, J. L., and Wardell, J. F., "The Scaled Thermal Explosion Experiment," in Proceedings of 12th International Detonation Symposium, San Diego, CA, (2002).
7 Tarver, C. M. and Tran, T. D., Combustion and Flame (2004) 50-62.
8 McClelland, M. A., Maienschein, J. L., and Nichols, A. L., Joint DoD/DOE Munitions Technology Development Program FY-01 Progress Report, Ignition and Initiation Phenomena: Cookoff Violence Prediction, Lawrence Livermore National Laboratory, (2002).
9 Bird, R. B., Stewart, W. E., and Lightfoot, E. N., *Transport Phenomena* (Wiley, 1960) 260-261.
10 . Dick, J. J., and Nartunez, A. R., Shock Compression of Condensed Matter-2001, Furnish, M. D., Thadhani, N. N., and Horie, Y, eds. CP-620, AIP Press, New York, 2002, pp 817.
11. Maienschein, J. L. and Chandler, J. B., Eleventh International Detonation Symposium, Office of Naval Research ONR 33300-5, Snowmass, CO, 1998, pp. 872-879.
12. Farber, D. L., Zaug, J. M., and Ruddle, C., Shock Compression of Condensed Matter-2001, Furnish, M. D., Thadhani, N. N., and Horie, Y, eds. CP-620, AIP Press, New York, 2002.
13. A. W. Campbell and Ray Engelke, 6th Symposium (International) on Detonation, White Oak, MD, August 1976
14 Holman, J. P., Heat Transfer (McGraw-Hill, 1976) 253-254.
15 Sharp, R., "Users Manual for ALE3D An Arbritrary Lagrange/Eulerian 3D Code System", Lawrence Livermore National Laboratory, (2003)
16 Yoh, J. J., McClelland, M. A., Maienschein, J. L., Wardell, J. F., and Tarver, C. M., "Simulating thermal explosion of cyclotrimethylenetrinitramine-based explosive: Model comparison with experiment," J. Appl. Phys. (2005) in press.
17 Yoh, J. J., McClelland, M. A., Maienschein, J. L., Wardell, J. F., "Towards a predictive thermal explosion model for energetic materials," J. Comp.-Aided Matls. Design (2005) 175-179.